Podosomes in osteoclast-like cells: structural analysis and cooperative roles of paxillin, proline-rich tyrosine kinase 2 (Pyk2) and integrin αVβ3

Martin Pfaff*,‡ and Pierre Jurdic

Ecole Normale Supérieure de Lyon, 46 allée d'Italie, 69364 Lyon Cedex 07, France
*Present address: Institut Albert-Bonniot, LEDAC (UMR5538), Faculté de Medecine, F 38706 La Tronche Cedex, France
‡Author for correspondence (e-mail: martin.pfaff@ujf-grenoble.fr)

Accepted 1 May 2001
Journal of Cell Science 114, 2775-2786 (2001) © The Company of Biologists Ltd

SUMMARY

Macrophages and osteoclasts develop unique contact sites with the extracellular matrix called podosomes. Podosomes have been associated with migratory and invasive cell characteristics, but a basic mechanism outlining their function is lacking. We have used chicken and human monocytes differentiating in vitro into osteoclast-like cells in the presence of RANKL-ODF to study these cytoskeletal structures. During the differentiation process, podosomes are redistributed from the cell body in early macrophages to the cell periphery in increasingly spread and multinucleated cells expressing high levels of integrin αVβ3. Immunofluorescence with anti-phosphotyrosine antibodies revealed increased tyrosine-phosphorylation at the basal tips of these podosomes. RANKL-ODF treatment reinforced the peripheral location of podosomes and initiated their partial fusion to larger F-actin-containing structures that displayed reduced levels of tyrosine phosphorylation. Paxillin and the FAK-related kinase Pyk2 colocalized with integrin αVβ3 in the juxtamembrane region surrounding individual podosomes. In lysates of macrophages and differentiated osteoclasts both paxillin and Pyk2 associated with synthetic and recombinant polypeptides containing the C-terminal region of the integrin β3 cytoplasmic domain. These in vitro interactions were direct and they were abolished by substitutions in the β3 integrin peptides known to disrupt integrin function in vivo. The marked adhesion-dependent tyrosine-phosphorylation of Pyk2 and paxillin however did not detectably alter their interaction with β3 tail peptides in cell lysates. Our results provide novel insight into the molecular architecture and the phosphorylation dynamics in podosomes. Moreover, they outline a novel potential mechanism for the recruitment of paxillin and Pyk2 to β3 integrin-dependent cell contacts.

Key words: Osteoclast, Podosome, Integrin, Cytoskeleton, Cell adhesion

INTRODUCTION

Cultured cells develop discrete sites of contact with the extracellular matrix, in which clustered transmembrane proteins, particularly of the integrin family of adhesion receptors, link extracellular matrix proteins to the actin cytoskeleton within the cell (Hynes, 1992). Focal adhesion plaques represent the most ubiquitous and well known of these contacts. They are characterized by their connection to easily detectable bundles of actin filaments, called stress fibers (Burridge and Chrzanowska-Wodnicka, 1996; Jockusch et al., 1995). Most cells additionally develop smaller peripheral contact sites (focal complexes) often associated with lamellipodia, which can develop into bona fide focal adhesions (Rottner et al., 1999). By contrast, only very few cell types form different, much less understood adhesion sites that consist of dot-shaped, F-actin-rich close contacts, which have been initially described in cells transformed by Rous sarcoma virus (RSV; David-Pfeuty and Singer, 1980) and later in monocyte-derived cells including macrophages (Marchisio et al., 1987) and osteoclasts (Marchisio et al., 1984). These cytoskeletal structures have been named 'rosettes', owing to their appearance as small black rings in interference reflection microscopy (IRM; David-Pfeuty and Singer, 1980). However the name 'podosomes', which denotes their foot-like appearance in electron-microscopy is now most commonly accepted (Tarone et al., 1985).

It has been recognized that podosomes share major structural components with focal adhesions, e.g. α-actinin, vinculin and talin (David-Pfeuty and Singer, 1980; Marchisio et al., 1984; Marchisio et al., 1987). Furthermore, both structures are sites of increased protein tyrosine phosphorylation (Tarone et al., 1985; Burridge and Chrzanowska-Wodnicka, 1996). On the other hand, proteins, like gelsolin (Yin, 1987) and fimbrin (T-plastin; Bretscher, 1981), which regulate actin filament organization, are enriched only in podosomes (Wang et al., 1984; Carley et al., 1986; Marchisio et al., 1984; Marchisio et al., 1987). Recent genetic evidence underlines the particular importance of two such proteins for podosome function in vivo, of gelsolin (Chellaiah et al., 2000) and WASP (Linder et al., 1999). These data suggest that the mechanisms linking cell adhesive contacts to the F-actin cytoskeleton are similar in focal adhesions and podosomes, but that both structures differ in the

mechanisms that regulate the microarchitecture of actin filaments.

Using time-lapse video and photobleaching techniques in RSV-transformed rat kidney cells microinjected with fluorescent α-actinin, Stickel and Wang (Stickel and Wang, 1987) observed that podosomes underwent rapid formation, movement and breakdown. Fluorescing α-actinin molecules were replaced in podosomes with a halftime of fluorescence recovery of 4 seconds, more than 10 times faster than in focal adhesions of non-transformed cells. Thus, podosomes are highly dynamic structures, that rapidly move and change shape and size. Chen and co-workers have noted that podosomes in RSV-transformed cells, but not focal adhesions in the non-transformed cells, colocalize with proteolytic activities that degrade extracellular matrix proteins (Chen et al., 1984; Chen, 1989). In transmission electron microscopic images, they associated these proteolytic activities with membrane protrusions, called invadopodia, formed adjacent to the rosette contact sites. Two other studies (Nitsch et al., 1989; Ochoa et al., 2000) have described invaginations of the plasma membrane reaching into the center of podosomes. These are associated with membrane transport phenomena, as indicated by the presence of the GTPase dynamin 2 (Ochoa et al., 2000), and might represent sites of local protease release. Moreover, podosomes co-distribute with matrix metalloproteinases in osteoclasts (Blavier and Delaissé, 1995; Sato et al., 1997). Therefore, podosomes appear to be structures that uniquely combine adhesive functions with proteolytic degradation of the extracellular matrix, characteristics that are especially important for highly invasive cells.

The adhesive mechanisms establishing the podosome contact with the extracellular matrix are not well understood. Experimental evidence that demonstrates a direct implication of integrins in podosome function is scarce compared with their well-established role in the formation of focal adhesion plaques (Burridge and Chrzanowska-Wodnicka, 1996). Yet integrins have been localized to podosomes that co-distribute either with F-actin (Marchisio et al., 1988; Nakamura et al., 1999) or with the plasma membrane region directly adjacent to it (Marchisio et al., 1988; Helfrich et al., 1996; Zambonin-Zallone et al., 1989). One study (Johansson et al., 1994) has localized a subpopulation of β1 integrin subunits that contain a phosphorylated tyrosine in its cytoplasmic domain in podosomes of RSV-transformed cells. In osteoclasts, podosomes are putative precursors of the sealing zone, a tight adhesion structure that seals the cells onto bone during resorptive activities (Väänänen and Horton, 1995). Osteoclasts express integrin αVβ3 as major integrin adhesion receptor, which is required for the formation of the sealing zone ex vivo and for bone resorbing activity in vivo (McHugh et al., 2000). However, it is highly questioned whether this integrin provides the adhesive link between the sealing zone and bone, because it could not be localized in this adhesive structure (Lakkakorpi et al., 1991; Helfrich et al., 1996; Väänänen et al., 2000). By contrast, several reports demonstrate an association of this integrin with podosomes in non-resorbing osteoclasts or osteoclast-like cells (Nakamura et al., 1999; Helfrich et al., 1996; Zambonin-Zallone et al., 1989).

We have decided to study podosomes in cells of the monocytic lineage, which represent the sole untransformed cell types forming podosomes. We observed the organization and the molecular architecture of these structures during the differentiation of human and chicken monocyte-derived precursor cells to bone-resorbing osteoclasts. This differentiation was initiated by the cytokine RANKL-ODF (ligand of receptor activator of NFκB-osteoclast differentiation factor; Yasuda et al., 1998; Anderson et al., 1997), which induced high expression levels of integrin αVβ3, reinforced the distribution of podosomes at the cell periphery, and initiated their partial fusion to larger F-actin-containing structures. We also observed changes in the distribution of tyrosine-phosphorylated proteins in the podosome zone, together with the terminal steps of differentiation. Moreover, we demonstrate the colocalization of integrin αVβ3 in the juxtamembrane region adjacent to podosomes with the non-receptor tyrosine kinase Pyk2 and the cytoskeletal adapter protein paxillin. Both of these latter proteins, especially paxillin, incorporated high amounts of phosphate into tyrosine residues during cell adhesion. Finally, we provide evidence from in vitro binding experiments pointing to a novel, direct interaction of both paxillin and Pyk2 with the C-terminal region of the integrin β3 tail. This interaction might be a crucial element in podosome function in osteoclast-like cells.

MATERIALS AND METHODS

Reagents

We used the following antibodies: mAb 23C6, directed against integrin αVβ3, was kindly donated by Dr M. Horton, London; mAbs clone 5 (anti-tensin), 21 (anti-zyxin), 11 (anti-Pyk2), 21 (anti-p130cas), 349 (anti-paxillin), 30 (anti-cortactin) were purchased from Transduction Laboratories; mAb BM-75.2 (anti-α-actinin) was from Sigma; mAb 4F11 (anti-cortactin) from Upstate Biotechnology; anti-phosphotyrosine mAbs were 4G10 (produced in our laboratory) and PY99 from Santa Cruz Biotech; mAb 327 (anti-pp60src) was donated by Dr J. Brugge, Boston; and mAb 3F3A5 (anti-WASP) was donated by Dr David Nelson (Bethesda, MD). The following antibodies were purchased from the Developmental Studies Hybridoma Bank maintained by the John Hopkins University, Iowa City: mAb 8e6 (anti-talin) developed by C. Otey and K. Burridge; and mAb VN3-24 (anti-vinculin) developed by S. Saga. Fluorescein- and peroxydase-labeled secondary antibodies were from Jackson Laboratories and rhodamine-phalloidin was from Molecular Probes. Human recombinant soluble RANKL-ODF was provided by Immunex (Seattle, WA) and human recombinant M-CSF was purchased from R&D SYSTEMS. David Schlaepfer (La Jolla, CA) kindly provided a pCDNA3.1 expression vector for Myc-tagged human full-length Pyk2.

Cell culture

Chicken monocytes were isolated from Ficoll-separated peripheral blood cells and cultured as described previously (Solari et al., 1995; Boissy et al., 1998). After 2 days of initial culture, adherent macrophages were trypsinized and replated onto coverslips or plastic dishes. For RANKL-ODF treatment, cells were cultured in αMEM containing 10% fetal calf serum (HyClone Laboratories) and 30 ng/ml RANKL-ODF for 2 to 5 days. Adherent human peripheral blood macrophages, similarly obtained from Ficoll-separated peripheral blood leukocytes, were cultured in αMEM, 10% fetal calf serum (HyClone Laboratories) and treated for 6-9 days with 50 ng/ml RANKL-ODF and 20 ng/ml M-CSF. Murine RAW 264.7 cells were obtained from ATCC (Rockville, Maryland) and cultured in DMEM, 10% fetal calf serum (HyClone Laboratories).

Immunofluorescence

Cells grown on glass coverslips were for a short period immersed in phosphate-buffered saline (PBS) and immediately fixed in 2.5% paraformaldehyde, 5% sucrose in PBS for 10 minutes at room temperature. Cells were permeabilized in 0.1% Triton X-100, 1 mM sodium orthovanadate in PBS for 5 minutes. After washing, coverslips were blocked with 1% bovine serum albumin, 1 mM sodium orthovanadate in PBS and incubated with first and secondary antibodies and rhodamine phalloidin in this same buffer. PBS-washed samples were mounted in Fluorsave™ (Calbiochem) containing 0.05% *p*-phenylenediamine and observed the next day with an epifluorescence microscope (Axioplan 2, Zeiss) equipped for confocal immunofluorescence analysis (LSM510, Zeiss).

Peptide and protein synthesis

Peptides were synthesized as described (Boissy et al., 1998). They consisted of N-terminally biotinylated penetratin peptide (RQIKIWFQNRRMKWKK), which was directly followed by integrin β cytoplasmic domain sequences (represented in Fig. 6A). Peptide purity was controlled by HPLC and their correct mass confirmed by electrospray mass spectrometry. Recombinant structural mimics of human integrin β1 and β3 tails were provided by David Calderwood and Mark Ginsberg (La Jolla, CA). These proteins consist of the full-length integrin cytoplasmic domains (Fig. 8) linked at their N terminus to a heptad-repeat and a His-Tag sequence, as described (Calderwood et al., 1999; Pfaff et al., 1998).

A pGEX-2TK™ vector for bacterial expression of glutathione-S-transferase-(GST)-linked human paxillin was kindly provided by Dr Mark Ginsberg (La Jolla, CA) with kind permission of Dr Ravi Salgia (Boston, MA). Recombinant GST-paxillin was produced in *Escherichia coli* strain DH5α (GIBCO Life Technologies) and purified on glutathione crosslinked agarose (Sigma) from bacterial lysates. Lysis and purification were performed in 20 mM Tris/HCl pH 8.0, 0.1% Triton X-100, 100 mM sodium chloride, 1mM EDTA, 1 mM DTT. Bound paxillin was eluted from glutathione beads with 20 mM reduced glutathione, 0.75 M Tris/HCl pH 9.6 and added to 1/2 volume of 1.5 M Tris/HCl pH 6.8.

A pEGB mammalian GST-fusion expression vector to produce GST-linked human Pyk2 N-terminal domain (amino acids 1-407) (GST-Pyk2-NT) was provided by David Schlaepfer (La Jolla, CA; Sieg et al., 2000). GST-Pyk2-NT was purified on glutathione agarose from lysates of transiently transfected 293T cells.

Immunoprecipitation and western blotting

After two short washes with PBS, cells were lysed in buffer A (50 mM Tris/HCl pH 7.4, 75 mM sodium chloride, 50 mM sodium fluoride, 40 mM sodium pyrophosphate, 1 mM sodium orthovanadate, 1 mM EDTA and protease inhibitors (Cømplete™, Boehringer Mannheim)) containing 1% Triton X-100, 0.5% sodium deoxycholate and 0.1% SDS. After 30 minutes on ice, lysates were cleared by centrifugation and agitated with Protein G Sepharose 4B (Sigma) for 1 hour at 4°C. Precleared lysates were incubated overnight with antibodies and Protein G Sepharose at 4°C. Immunoprecipitates were washed five times with buffer A containing 1% Triton X-100, 0.5% sodium deoxycholate and 0.1% SDS, and processed for SDS polyacrylamide electrophoresis followed by electrotransfer onto nitrocellulose (Amersham). Transfer efficiency was verified by Ponceau S staining. Nitrocellulose membranes were blocked overnight with 100 mM Tris/HCl pH 7.4, 150 mM sodium chloride containing either 5% fat-free milk powder (Régilait, France) or 3% bovine serum albumin, 0.1% Tween 20 (for incubations with anti-phosphotyrosine mAbs). After incubations with first and peroxydase-coupled secondary antibodies, bound antibodies were detected by chemiluminescence (ECL, Amersham).

Affinity precipitation with peptides

For peptide binding experiments, cell lysates were prepared in buffer A containing 1% Triton X-100, 0.2% sodium deoxycholate. Cleared lysates were diluted with one volume buffer A and incubated with biotinylated peptides prebound to crosslinked streptavidin agarose (Sigma) overnight at 4°C. After five to six washes with buffer A, containing 0.5% Triton X-100 and 0.1% sodium deoxycholate, bound proteins were eluted by boiling in reducing sample buffer for SDS gel electrophoresis. The presence of equal amounts of the different peptides in each experiment was verified on Coomassie-stained 15% SDS polyacrylamide gels and bound proteins were identified by specific antibodies on 8-10% SDS polyacrylamide gels transferred to nitrocellulose. Binding to recombinant GST, GST-paxillin and GST-Pyk2-NT was performed under identical conditions, except that 0.5 mM DTT and 2 mg/ml bovine serum albumin were added to the binding buffer. Recombinant structural mimics of integrin β tails were used prebound to a Ni^{2+}-resin (Novagen) as described (Pfaff et al., 1998). To maintain their interaction with the resin, EDTA in buffer A had to be replaced with 1 mM $CaCl_2$ and 2 mM $MgCl_2$ throughout the experiment.

Digital image processing

Confocal images, scanned immunofluorescence photographs, as well as autoradiograms of western blots and scans of Coomassie Blue stained SDS-PAGE gels were digitally processed using the program Adobe Photoshop for the layout of the figures.

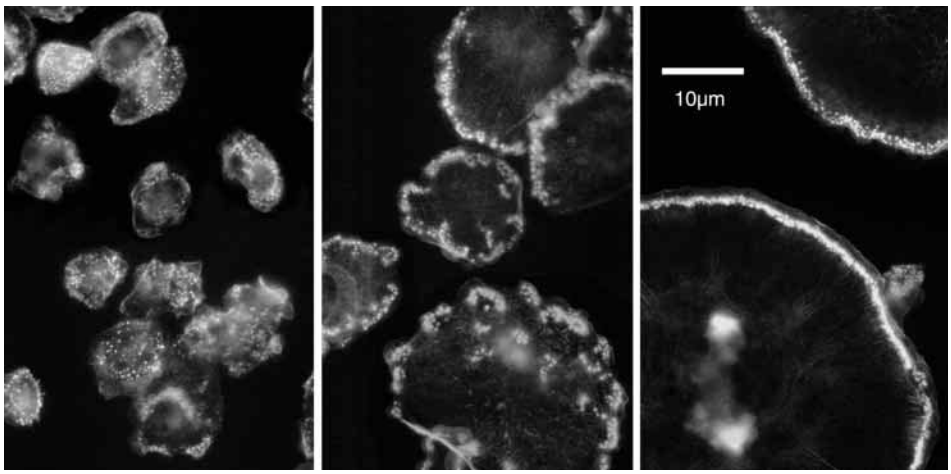

Fig. 1. The actin cytoskeleton in chicken osteoclast precursors during in vitro osteoclast differentiation. After an initial trypsinization (see Materials and Methods), macrophage-like cells were cultured on glass coverslips for one day (left panel) or for additional four days in the absence (middle panel) or presence (right panel) of RANKL-ODF. Subsequently, cells were fixed, permeabilized, stained with rhodamine-phalloidin and photographed on a Zeiss immunofluorescence microscope. Note the profound changes in the cellular distribution and in the density of podosomes. Scale bar: 10 μm.

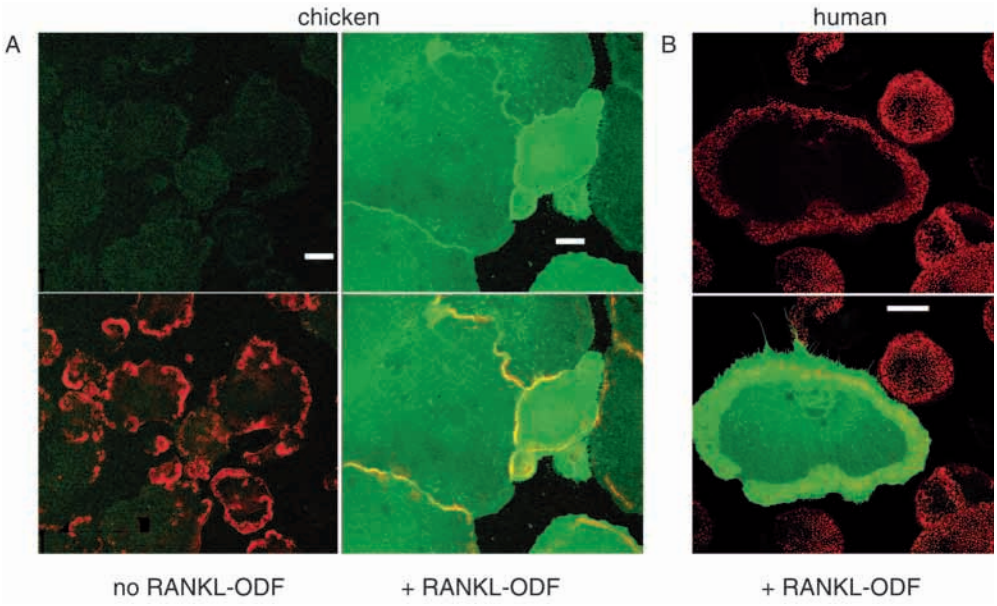

Fig. 2. Expression of integrin αVβ3 induced by RANKL-ODF treatment. (A) Chicken peripheral blood-derived macrophages were cultured on glass coverslips for four days in the presence (right panels) or absence (left panels) of RANKL-ODF (see Materials and Methods). Cells were fixed, permeabilized and stained with the monoclonal antibody 23C6 (green) and rhodamine-phalloidin (red). Confocal images were acquired using identical channel settings for αVβ3 detection and were equally processed in Adobe Photoshop to ensure comparable detection of αVβ3 expression. Upper panels, 23C6-staining only; lower panels, 23C6 + rhodamine phalloidin staining. (B) Human osteoclast obtained after a nine day treatment of peripheral blood monocytes with RANKL-ODF. Staining was performed as in A and revealed by confocal microscopy. Upper panel, rhodamine phalloidin-staining (red); lower panel, 23C6- (green) + rhodamine phalloidin-staining. Note the nearly complete absence of integrin αVβ3 on cells that were not treated with (A, left panels) or that did not visually respond to (B) the osteoclastogenic factor RANKL-ODF. Scale bar: 20 μm).

RESULTS

Cytoskeletal actin organization during the macrophage-osteoclast transition

Chicken peripheral blood monocytes were seeded onto plastic dishes and cultured in the absence or presence of the osteoclast differentiation factor RANKL-ODF. Within the first days of culture, monocytes adhered and spread out developing podosomes as major dot-like structures labeled by phalloidin (Fig. 1). At this early stage, podosomes were distributed throughout the basal cell body (Fig. 1, left panel). During continued culture cell sizes increased by cell fusion and spreading, and podosomes became more and more limited to peripheral cell regions. In the absence of RANKL-ODF the sizes of the moderately multinucleated cells remained within 20-80 μm and podosomes appeared in irregular and interrupted peripheral rings or loops, possibly representing local extensions of the plasma membrane (Fig. 1, middle panel). RANKL-ODF treatment for 2-4 days led to larger, more multinucleated cells (up to several hundred μms) with a smooth periphery lined by a band of tightly packed podosomes (Fig. 1, right panel). These podosomes showed an increasingly dense phalloidin-staining and, occasionally, individual actin spots fused to larger F-actin containing structures (Fig. 3B,C). Similar changes in the distribution of podosomes were observed during RANKL-ODF/M-CSF-induced differentiation of human peripheral blood monocytes (Figs 2B, 3C, 5). Human osteoclast precursors generally contained much more podosomes, but only a reduced number of osteoclasts were generated in vitro compared with the chicken cells (Fig. 2B). RANKL-ODF addition increased the expression of integrin αVβ3 from hardly detectable to moderate or extremely high levels in chicken (Fig. 2A), as well as in human osteoclast precursors (Fig. 2B; see also Quinn et al., 1998). The highly expressed integrin was distributed throughout the osteoclast plasma membrane, including in the peripheral podosome zone, where it appeared especially enriched (Figs 2, 5). In experiments performed with RANKL-ODF-differentiated chicken osteoclasts cultured for 5-6 days on dentine slices, we revealed their capacity to resorb bone (P. Boissy, O. Destaing, M. P. and P. J., unpublished). Thus, the presence of podosomes is characteristic for all differentiation stages during the macrophage-osteoclast transition, but their increased density at the cell periphery associated with high expression of the integrin αVβ3 reflects differentiation towards a bone-resorbing osteoclastic cell phenotype.

Podosome-associated tyrosine phosphorylation

To gain insight into the mechanisms that regulate podosome architecture and function, we have analyzed the association of tyrosine-phosphorylated proteins with these cytoskeletal structures during in vitro osteoclast differentiation. The major structures labeled by monoclonal anti-phosphotyrosine antibodies at all stages of differentiation were indeed podosomes (Fig. 3). Podosome-associated phosphotyrosine predominantly localized to the extracellular substrate-oriented podosome tips in early macrophages and in non-RANKL-ODF-treated cells (Fig. 3). This was especially evident in confocal images scanned in the *z*-axis, that sectioned individual podosomes in their centers (Fig. 3A,C, insets). However, the particularly F-actin-rich podosomes in RANKL-ODF treated osteoclast-like cells showed a reduced phospho-tyrosine staining (Fig. 3B,C, arrows in right-hand panels). Only the podosomes located at the side of the podosome ring facing the cell-centers were strongly stained at the tips (Fig. 3B,C, arrowheads in righthand panels). Reduced phospho-tyrosine staining of particularly large, F-actin-rich podosomes was also occasionally observed in non-RANKL-ODF-treated cells (see

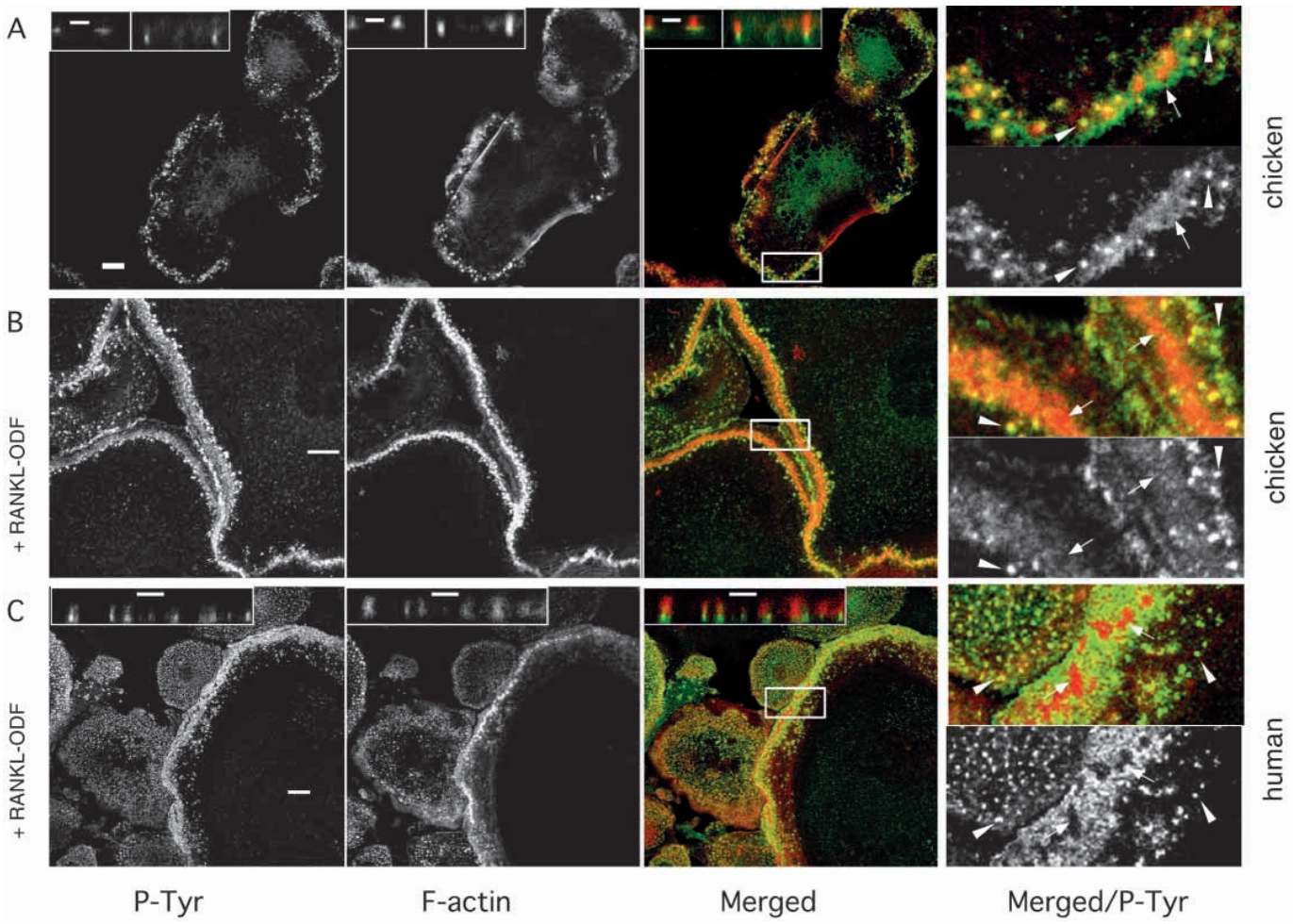

Fig. 3. Phosphotyrosine-detection in podosomes. Chicken (A,B) or human (C) osteoclast precursors cultured in the absence (A) or presence (B,C) of RANKL-ODF were double-stained with the antiphosphotyrosine antibody 4G10 and rhodamine-phalloidin and analyzed by confocal microscopy. (B) The cell peripheries of three chicken osteoclasts, which surround an undifferentiated mononuclear cell located at the upper left side. 4G10 and rhodamine staining are depicted separately and merged (4G10, green; rhodamine phalloidin, red). Insets at the upper left of panels in A and C are examples of high power views of podosomes obtained by scanning in the *z*-axis to show the bright phosphotyrosine signal at podosome tips. The bottom side of these insets corresponds to the cell side which is in contact with the extracellular substrate. Panels at the far right are fivefold magnifications of image regions marked by rectangles in the adjacent panels. Merged channels (upper half) and the 4G10 channel alone (bottom half) are represented. Arrows in the right-hand panels indicate cases where strongly rhodamine-stained structures did not co-distribute with a strong phosphotyrosine staining. Arrowheads indicate co-distribution of strong phosphotyrosine and strong F-actin signals. Scale bars: 10 μm in A,B; 2 μm in insets.

arrow in Fig. 3A, right-hand panel). These variations in the association of podosomes with tyrosine-phosphorylated proteins indicate a functional specialization of the podosome ring during RANKL-ODF-induced differentiation, which remains to be further elucidated.

Adhesion-dependent tyrosine phosphorylation in cellular lysates

To identify podosome proteins phosphorylated on tyrosine in a cell adhesion-dependent manner, we biochemically analyzed cellular lysates in western blotting with anti-phosphotyrosine antibodies. A distinct profile of tyrosine-phosphorylated proteins with major bands at 60, 70 and 85, and between 110 to 130 kDa was detected in lysates of adherent osteoclast precursors (Fig. 4). This profile was essentially unaffected during RANKL-ODF-induced differentiation (Fig. 4A). Tyrosine phosphorylation was strongly reduced in lysates of cells kept in suspension for 2 hours, but reappeared during subsequent cell adhesion in a time course reflecting the extent of cell spreading (Fig. 4B). The major tyrosine phosphorylated protein migrating at 70 kDa in SDS-PAGE gels was identified as paxillin (Fig. 4C). Because immunoprecipitation with anti-phosphotyrosine antibodies did not markedly reduce paxillin levels in the lysates, we conclude that only a small portion of paxillin was actually phosphorylated on tyrosine (Fig. 4D). In similar experiments, we detected adhesion-dependent tyrosine phosphorylation of the 115 kDa protein kinase Pyk2 (Fig. 4E) and of p130cas (data not shown). We also noted that the band at 60 kDa contained tyrosine-phosphorylated pp60c-src (data not shown), which remained markedly tyrosine phosphorylated in the suspended cells (Fig. 4B,E). So far, we were unable to identify the prominent tyrosine-phosphorylated protein

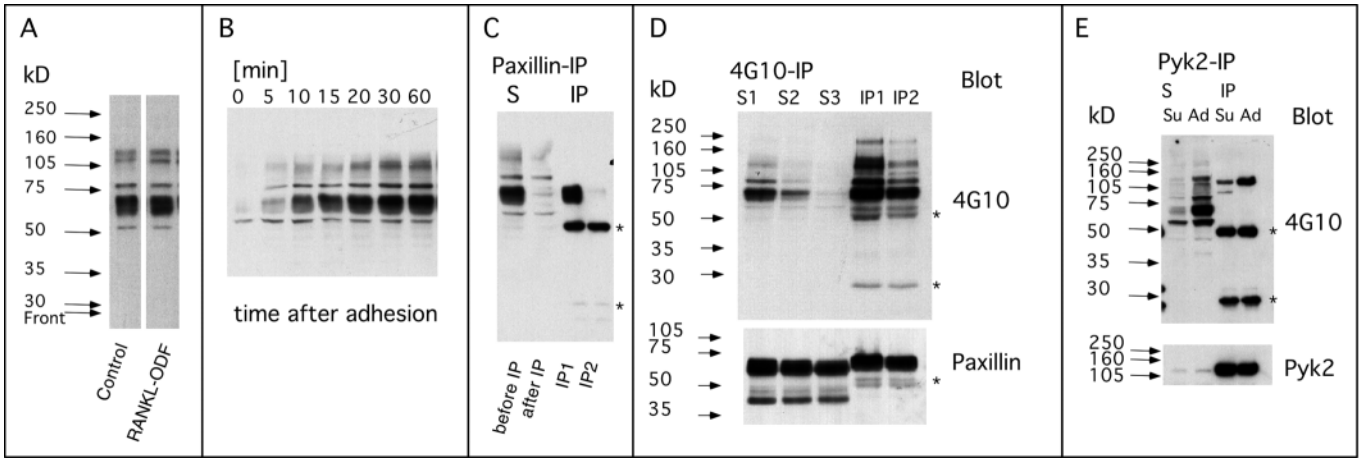

Fig. 4. Tyrosine-phosphorylated proteins in osteoclast-like cells. (A) Tyrosine-phosphorylated proteins in lysates of chicken osteoclast precursors cultured for 4 days in the absence or presence of RANKL-ODF were identified on immunoblots with the antibody 4G10 (an identical protein profile was revealed using the anti-phosphotyrosine antibody, mAb PY99 (see Fig. 6C)). Major bands were detected at 60, 70, 85 and 110-130 kDa. (B) Chicken osteoclast-like cells were trypsinized and kept in suspension for 2 hours at 37°C. Subsequently, the cells were seeded onto plastic coated with serum-containing culture medium and lysed after the indicated times. Equal amounts of lysate protein were added to each lane and analyzed by immunoblotting with monoclonal antibody 4G10. (C) Lysates of adherent chicken osteoclast-like cells were immunoprecipitated twice with anti-paxillin antibodies. Lysate supernatants (S) obtained before the first or after the second round of immunoprecipitation as well as the two immunoprecipitates (IP) were analyzed by immunoblotting with antiphosphotyrosine antibody 4G10. (D) Lysates of chicken osteoclast-like cells were subjected to two rounds of immunoprecipitation with antiphosphotyrosine antibody 4G10 and analyzed by western blotting with 4G10 or anti-paxillin antibodies. Lysate supernatants obtained before the first (S1), and before (S2) and after (S3) the second round of immunoprecipitation, as well as the two immunoprecipitates (IP1, IP2) are shown. Note the mobility shift of tyrosine-phosphorylated paxillin in the immunoprecipitates and the disappearance of a slower mobility fraction of paxillin in the supernatants of the immunoprecipitations. However, this fraction represents only a minor subpopulation of total paxillin. (E) Chicken osteoclast-like cells were trypsinized, kept in suspension (Su) for 2 hours or subsequently adhered (Ad) to serum-coated plastic for 40 minutes. Lysates of these cells were immunoprecipitated with anti-Pyk2 antibodies and analyzed by western blotting using 4G10 and anti-Pyk2 antibodies. S, lysate supernatants; IP, immunoprecipitates; asterisks mark the position of immunoglobulin chains in the immunoprecipitates, which were detected by the secondary antibodies.

migrating at 85 kDa. In conclusion, cell adhesion and spreading of osteoclasts and osteoclast precursors result in high-level tyrosine phosphorylation of a characteristic set of proteins, most notably, however, of a minor subpopulation of paxillin molecules.

Colocalization of integrin αVβ3, paxillin and Pyk2 in the podosome zone

We next analyzed the precise cellular location of podosome proteins by immunofluorescence (Fig. 5). Both paxillin and Pyk2 accumulated in the zone containing podosomes, but they were essentially confined to regions between the individual F-actin-containing core structures of podosomes (Fig. 5). Confocal images scanned in the *z*-axis narrowed down their location as being close to the extracellular substrate-oriented plasma membrane between the podosomes (Fig. 5, insets in left panels). A broader analysis showed that most of the proteins known to associate with focal adhesion plaques in other cells, like talin, vinculin, α-actinin, zyxin, tensin, p130cas and the integrin αVβ3, share a very similar subcellular location with paxillin and Pyk2 in the podosome zone (Fig. 5, and data not shown). A different distribution was observed for the src-substrate cortactin, which colocalized with the F-actin core of podosomes in horizontal confocal sections (resulting in yellow podosomes in images with merged F-actin and cortactin channels, Fig. 5, bottom panels). Vertical confocal sectioning (Fig. 5, inset in bottom left panel) revealed its preferential location in the basal tips of podosomes. A similar distribution was observed for the protein WASP (data not shown). Thus, the subcellular location of the proteins previously identified as major substrates of adhesion-dependent tyrosine phosphorylation (Fig. 4) was to some extent different from the subcellular structures stained during immunofluorescence with anti-phosphotyrosine antibodies (Fig. 3). Most notably, the prominent phosphotyrosine signal detected on the basal tips of podosomes (Fig. 3) corresponded best to the distribution of cortactin, but much less to that observed for paxillin, Pyk2 and integrin αVβ3 (Fig. 5). However, we could not detect adhesion-dependent phosphorylation on tyrosine in immunoprecipitates of cortactin. Moreover, although cortactin migrates as a 85 kDa band in SDS-PAGE gels, its immunodepletion from the cell lysates did not remove the major tyrosine-phosphorylated 85 kDa band (see Fig. 4; data not shown). Hence, an as yet unidentified protein might be responsible for the phosphotyrosine signal detected in situ on the podosome tips or, alternatively, the small subpopulation of paxillin molecules, which is actually phosphorylated on tyrosine (Fig. 4D), might be located close to the basal podosome tips.

Pyk2 and paxillin interact with the integrin β3 cytoplasmic tail

To gain insight into molecular interactions that link adhesion receptors to the particular actin cytoskeleton in macrophages

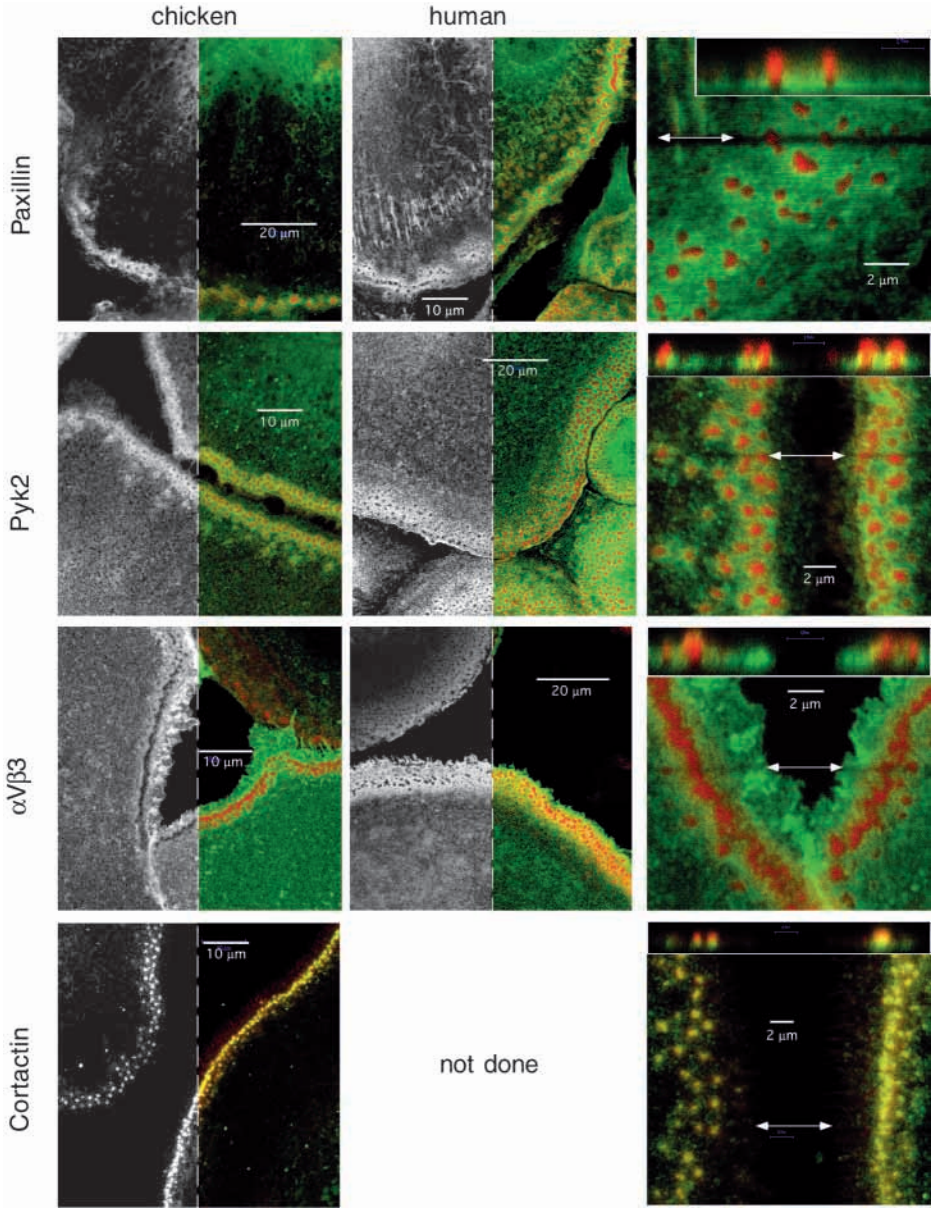

Fig. 5. Distribution of paxillin, Pyk2, integrin αVβ3 and cortactin in the podosome zones of chicken and human osteoclast-like cells. Confocal immunofluorescence images of cells double-stained with rhodamine phalloidin (red) and with antibodies for paxillin, Pyk2, αVβ3 or cortactin (green in colored images or white in grayscale images) are shown. Right-hand panels are high-power views, which were also scanned in the *z*-axis at positions indicated by the double-arrows. These *z*-axis scans are shown on top of these panels with the extracellular substrate-facing cell side oriented towards the bottom of the images. Note the co-distribution of paxillin, Pyk2 and αVβ3 around and between, but not within, the F-actin core structures of podosomes. By contrast, cortactin shows an inverse distribution, i.e. colocalization with F-actin in *xy*-scans, but appears also orientated towards the basal podosome side, as indicated by the separation of red (F-actin) and green (cortactin) channels in the inset scanned in the *z*-axis.

and osteoclast-like cells, we performed affinity precipitation experiments with peptides containing the C-terminal third of integrin β cytoplasmic domains (Fig. 6A). In a previous study, we have shown that such a peptide containing the 17 C-terminal amino acids of the chicken integrin β3 tail, which is rendered membrane permeable by its coupling to penetratin (Derossi et al., 1994), blocked the spreading of cultured macrophages expressing high levels of αVβ3 (Boissy et al., 1998). When incubated with a lysate of macrophages or osteoclast-like cells, this peptide precipitated high amounts of two tyrosine-phosphorylated proteins, which were identified as paxillin and Pyk2 (Fig. 6B,D). Two other cytoskeletal proteins, talin and vinculin, did not bind to this peptide (Fig. 6B and data not shown). Peptides containing single amino-acid substitutions (S-752-P; Y-759-A), previously reported to compromise β3 integrin function (Chen et al., 1992; O'Toole et al., 1995; Ylänne et al., 1995; Schaffner-Reckinger et al., 1998) or a peptide containing the homologous region of the integrin β1 tail bound these proteins only very weakly or not at all (Fig. 6B). Experiments with lysates of suspended and attached cells indicated that the interactions with both paxillin and Pyk2 did not correlate with the extent of adhesion-triggered tyrosine phosphorylation (Fig. 6C). Moreover, Pyk2 binding to the β3 cytoplasmic tail was unaffected by immunodepleting cell lysates for paxillin (Fig. 6D). This indicates that it was independent of the known interaction between Pyk2 and paxillin (Schaller and Sasaki, 1997). Finally, binding of both latter proteins to the β3 tail was observed in additional experiments using the chicken β3-tail peptide (shown in Fig. 6A) with lysates of a murine monocyte-derived cell line RAW 264.7 and of human 293T cells transfected with human Pyk2 (data not shown).

Purified glutathione-S-transferase fusion proteins of full-length human paxillin and of the N-terminal part of Pyk2 (amino acids 1-407) also strongly bound to the unmodified integrin β3 tail peptide, whereas glutathion-S-transferase

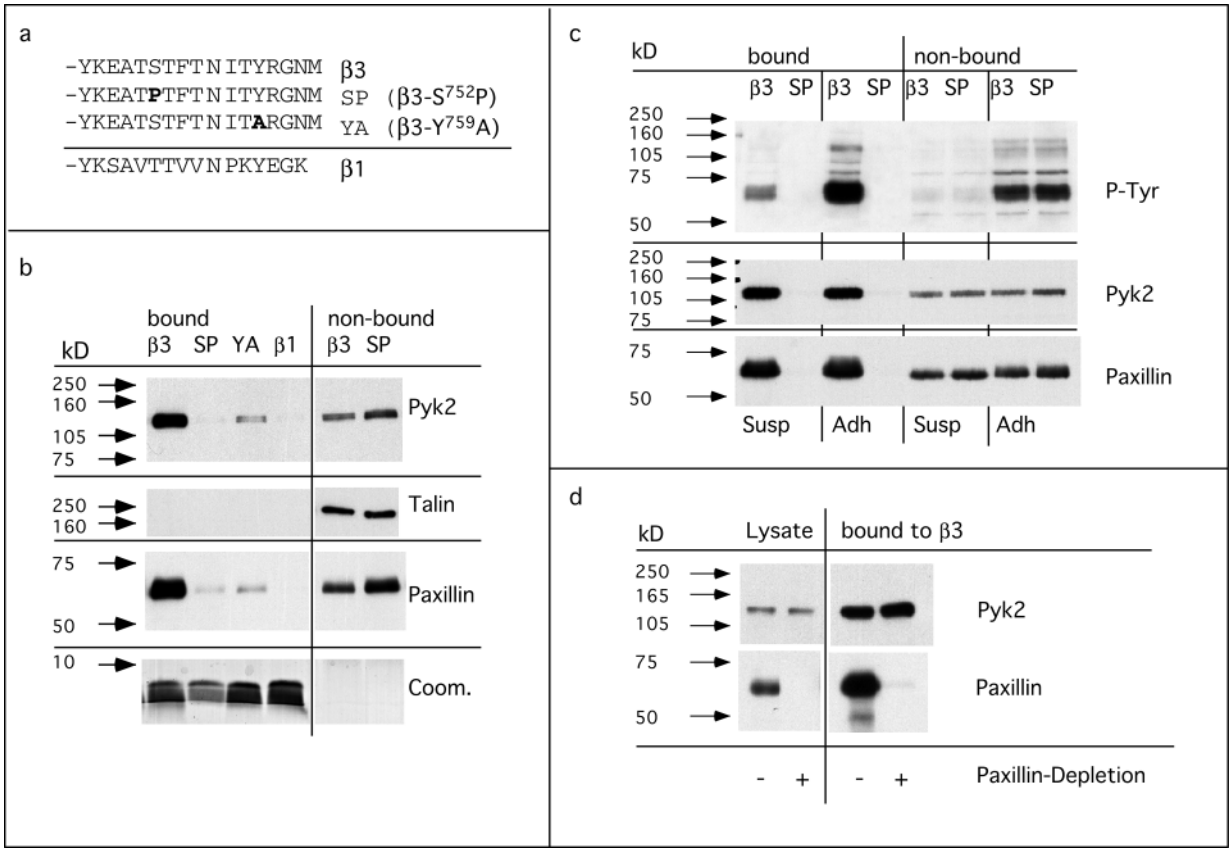

Fig. 6. Binding of paxillin and Pyk2 to synthetic peptides containing the C terminus of the integrin β3 cytoplasmic domain. (A) Integrin-derived sequences of the peptides: the C terminus of the chicken integrin β3 tail, two variants of this sequence containing single amino acid substitutions ($S^{752}P$ (SP), $Y^{759}A$ (YA)), and the corresponding region of the integrin β1 tail were linked at their N termini to penetratin, which was itself biotinylated at its N terminus. (B) Affinity precipitation experiment performed with these peptides and cell lysates of chicken osteoclast precursors. Proteins bound to the peptides were eluted together with these peptides into reducing sample buffer for SDS-polyacrylamide electrophoresis, and analyzed by immunoblotting with antibodies against talin, Pyk2 and paxillin. Peptides (M_r approx. 4.5 kDa) were detected on separate Coomassie-stained 15% SDS-polyacrylamide gels (Coom.). Supernatants of the binding reaction were also analyzed (unbound). Note the partial depletion in the β3-unbound fraction of Pyk2 and paxillin, but not of talin. (C) Affinity precipitation with wild-type and $S^{752}P$-mutated integrin β3-tail peptides performed with chicken osteoclast-like cells that had been lysed either after 2 hour suspension culture (Susp) or after 40 minutes adhesion to serum-coated plastic (Adh). Bound and non-bound fractions were analyzed by immunoblotting with an antiphosphotyrosine mAb (PY99), or with antibodies against paxillin and Pyk2. Note that equal amounts of paxillin and Pyk2 were bound, although the levels of tyrosine phosphorylation differed strongly in the lysates of suspended versus adhered cells. (D) Affinity precipitation with the β3-tail peptide performed with lysates of chicken osteoclast-like cells. Half of the lysates had been subjected to two rounds of immunoprecipitation with an anti-paxillin monoclonal antibody before the incubation with the β3-tail peptide. Lysates and bound fractions were analyzed by immunoblotting with antibodies against Pyk2 and paxillin. Note that equal amounts of Pyk2 bound from paxillin-containing and paxillin-depleted lysates.

alone showed negligible binding (Fig. 7). Therefore, both interactions appear to be direct.

To further confirm these results, we used recombinant structural mimics of integrin β tails containing full-length human cytoplasmic domains in similar experiments (Fig. 8; Pfaff et al., 1998). These studies revealed again significant binding of both paxillin and Pyk2 in lysates of chicken osteoclast precursors (Fig. 8) and in mammalian cell lines (data not shown) to the integrin β3 cytoplasmic domain. We also noted somewhat reduced, but still significant binding of Pyk2 and paxillin to the full-length β1 tail (Fig. 8). As expected from other studies, both full-length β1 and β3 tails bound to talin, and talin binding was disrupted by tyrosine-alanine mutations in their membrane-proximal NPXY motifs (Pfaff et al., 1998; Calderwood et al., 1999; Fig. 8). Interestingly, this same mutation also abolished paxillin and Pyk2 binding to the integrin β3 tail, but not to the integrin β1 tail (Fig. 8), suggesting differing binding requirements for β1 and β3 tails. Therefore, these data provide evidence for novel and direct interactions of the integrin β3 tail C-terminal region with paxillin and Pyk2.

DISCUSSION

We have analyzed the podosome organization in peripheral blood monocyte-derived cells during their in vitro differentiation to osteoclasts. We present the following observations.

(1) Osteoclast differentiation induced by RANKL-ODF is

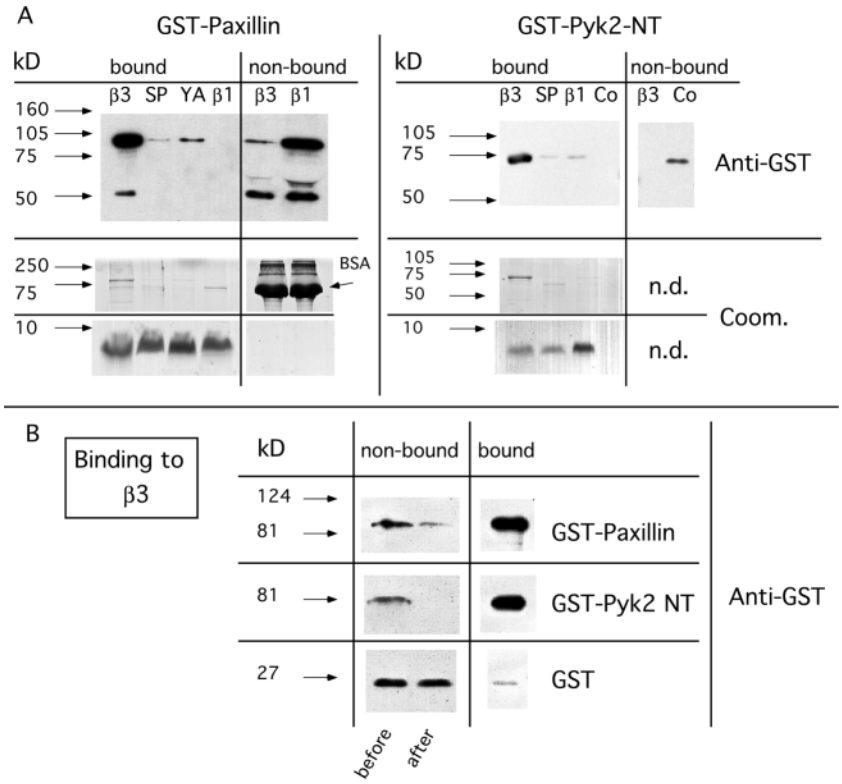

Fig. 7. (A) Binding of synthetic peptides (see Fig. 6A) to purified GST-fusion proteins of paxillin (expected M_r approx. 95 kDa) and of the N-terminal domain (amino acids 1-407) of human Pyk2 (expected M_r approx. 70 kDa). Bound and unbound proteins were analyzed by immunoblotting with an anti-GST antibody as well as on Coomassie-stained 15% SDS-polyacrylamide gels. Note the depletion of GST-fusion proteins in the supernatants incubated with the β3-tail peptide. Note also the nearly complete absence of bovine serum albumin in the bound fractions, which was present in a very large excess over GST-fusion proteins in the binding reactions. (Co, control resin consisting of streptavidin agarose without any added peptide; n.d., not done). (B) Comparison of GST, GST-paxillin and GST-Pyk2NT binding to the β3-tail peptide. Note the depletion in the unbound fractions of GST-Pyk2NT and GST-paxillin after binding. GST proteins were calibrated to give comparable signals in the supernatants by detection with Anti-GST antibody.

accompanied by profound changes in the distribution, density and tyrosine phosphorylation of podosomes. These changes could correlate with the acquisition of novel podosome functions related to their role as precursors of the sealing zone in bone-resorbing osteoclasts.

(2) The protein paxillin is the major acceptor of cell adhesion-induced tyrosine phosphorylation in early and late osteoclast precursors. It colocalizes with the integrin αVβ3 and the protein kinase Pyk2 in the juxtamembrane region directly adjacent to podosomes of human and chicken osteoclast-like cells.

(3) Both paxillin and Pyk2 bind in vitro to the C-terminal 17 amino acids of the integrin β3 tail. Both of these interactions are direct and not affected by adhesion-induced tyrosine phosphorylation of paxillin and Pyk2. Moreover, they can be observed in lysates of chicken as well as of mammalian cells.

Our results suggest key roles of these three proteins in the regulation of cell adhesion-triggered cytoskeletal organization and signal transduction in podosome-containing cells derived from the monocytic lineage.

During RANKL-ODF-induced osteoclast differentiation of peripheral blood monocytes, podosomes formed early in macrophage-like precursor cells. At this stage, podosomes were found throughout the basal cell body (Fig. 1). During subsequent culture, the cells increasingly spread and began to fuse; concomitantly, their podosomes redistributed towards the cell periphery. This change in podosome distribution might reflect a change in the mechanism of podosome-mediated cell movement: we have observed that mononuclear osteoclast precursors migrate as ‘whole cells’, whereas the movement of large multinucleated osteoclast precursors rather consists in

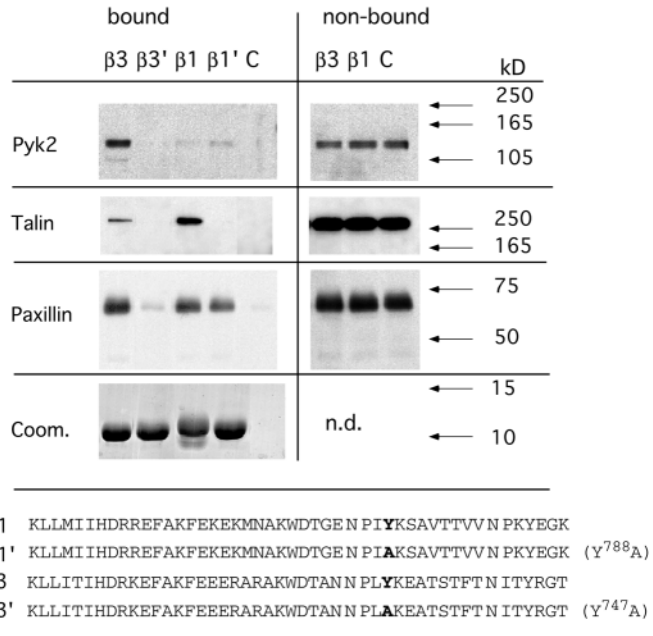

Fig. 8. Binding of recombinant structural mimics of human integrin β1 and β3 cytoplasmic tails to proteins in lysates of chicken osteoclast precursor cells. Integrin sequences of the recombinant proteins are depicted at the bottom, including those containing a tyrosine-alanine point mutation at a conserved NPXY motif. Via an N-terminal His-Tag sequence, these proteins were bound to a Ni^{2+}-resin and incubated with cell lysates. Bound cellular proteins were eluted together with the recombinant proteins from the resin and analyzed by western blotting with antibodies against Pyk2, Talin and Paxillin. Coomassie Blue staining (Coom.) was used to verify that comparable amounts of recombinant proteins were present in each experiment. Supernatants of the binding reactions were also analyzed (non-bound). (C, control Ni^{2+}-resin used without any added His-tagged protein; n.d., not done).

extensions and retractions of peripheral cell parts (S. Ory and P. J., unpublished). In these osteoclast precursors, the podosome tips facing the extracellular substrate are strongly enriched in tyrosine-phosphorylated proteins. RANKL-ODF-treatment reinforced the peripheral podosome distribution and led to more tightly packed podosomes, which occasionally fused to larger F-actin containing aggregates. This possibly reflects initial differentiation of the podosome ring to a functional sealing zone, which normally forms only in bone-resorbing osteoclasts (Väänänen and Horton, 1995). The densely packed podosomes in RANKL-ODF-treated cells contained reduced amounts of phosphotyrosine, which did not appear to be topologically associated with the prominent F-actin containing structures. Hence, the osteoclastogenic factor RANKL-ODF induced discrete alterations in the microarchitecture of podosomes and in their association with tyrosine-phosphorylated proteins.

However, a very similar set of proteins in cell lysates was phosphorylated on tyrosine in a cell-adhesion-dependent manner in both RANKL-ODF-treated and untreated cells (Fig. 4A). Thus, changes in the cellular distribution (Fig. 3) rather than in the tyrosine phosphorylation of these proteins predominate during osteoclast differentiation. Most of the phosphotyrosine generated in adherent and spread macrophages or osteoclasts was detected in the LIM protein paxillin (Turner, 1994a), a scaffolding protein with binding sites for many proteins, including the cytoplasmic protein tyrosine kinases FAK, Pyk2 and c-src (Schaller and Sasaki, 1997; Weng et al., 1993; Sabe et al., 1994), the protein-tyrosine phosphatase PTP-Pest (Shen et al., 1998), and the cytoskeletal protein vinculin (Turner and Miller, 1994). Paxillin also provides a link between regulators of p21 GTPases and adhesion complexes by its binding to a protein complex containing the p21 GTPase-activated kinase (PAK) and the guanine nucleotide exchange factor PIX (Turner et al., 1999). Thus, paxillin is in a key position to regulate adhesion-dependent cytoskeletal organization and signal transduction. So far, its role in osteoclast adhesion and in podosome function has not been thoroughly addressed, although several recent studies noticed its colocalization with F-actin, vinculin, Pyk2 and p130cas in the sealing zone of mouse osteoclasts (Lakkakorpi et al., 1999; Duong et al., 1998). In addition, a 70 kDa protein, probably identical to paxillin, has been identified as predominant tyrosine-phosphorylated adhesion substrate in human monocytes (Lin et al., 1994). We now identify paxillin as the major tyrosine-phosphorylated protein in differentiating osteoclasts. It co-distributes with the integrin αVβ3, the non-receptor tyrosine kinase Pyk2 and with many other proteins, which are typically found in focal adhesion complexes, in the membrane-proximal region immediately adjacent to podosomes (Fig. 5; M. P. and P. J., unpublished; see also Lakkakorpi et al., 1999; Duong et al., 1998; Nakamura et al., 1999; Helfrich et al., 1996; Zambonin-Zallone et al., 1989; David-Pfeuty and Singer, 1980; Marchisio et al., 1984; Marchisio et al., 1987).

Cell adhesion phenomena associated with podosomes are not very well characterized. It remains to be demonstrated in molecular detail, how podosomes contact the extracellular substrate. IRM techniques have revealed that podosomes contact the substrate within a small ring (a rosette) co-distributing with the protein vinculin around the central actin core (David-Pfeuty and Singer, 1980; Marchisio et al., 1984). This topology of the contact zone of a podosome is consistent with the subcellular location of paxillin, Pyk2 and the major osteoclast integrin, αVβ3, revealed in this study. It implies that strong integrin-dependent adhesion and cytoskeletal linkage occur predominantly in this delimited region, where adhesion receptors most closely approach the central actin-rich podosome core. Moreover, these locally restricted cell adhesive contacts could also trigger the strong protein tyrosine phosphorylation that we observed at the podosome tips. This phosphotyrosine staining observed in situ could correspond to the predominant tyrosine phosphorylation of paxillin detected in lysates of adherent osteoclast precursors, assuming that only a small subpopulation of paxillin molecules located near the podosome contact zone is involved.

We report for the first time that the 17 C-terminal residues of the integrin β3 chain strongly and directly bind to both paxillin and Pyk2 (Figs 6-8). An interaction between paxillin and integrin β cytoplasmic domains has been suggested in earlier studies (Schaller et al., 1995; Tanaka et al., 1996). Schaller et al. reported paxillin binding to the membrane-proximal regions of integrin β1, β2 and β3 tails, but they did not provide evidence that the interaction was direct (Schaller et al., 1995). Tanaka et al. demonstrated direct paxillin binding to the integrin β1 cytoplasmic domain (Tanaka et al., 1996). Consistent with the former studies, we detected paxillin binding to full-length β1 tails, which was not abolished by a point mutation adjacent to and not overlapping the proposed binding motif (Schaller et al., 1995; Fig. 8). In contrast, our results show that paxillin interacts in a clearly different way with the integrin β3 tail. A peptide consisting of its 17 C-terminal amino acids alone contains strong paxillin binding activity and mutations at three critical positions in its C-terminal region abrogate this interaction. The serine(752)-proline mutation has been identified in a patient with Glanzmann's thrombasthenia and resulted, like the tyrosine-alanine mutations at positions 747 and 759, in compromised capacities of the integrin to become competent for ligand binding, to localize to focal adhesion plaques and to promote cell spreading (Chen et al., 1992; O'Toole et al., 1995; Ylänne et al., 1995; Schaffner-Reckinger et al., 1998). Hence, our results provide a potential molecular explanation for at least some of the defects observed with these mutants, notably those that interfere with cell spreading and focal adhesion localization.

We also observed strong binding of the protein kinase Pyk2 to the integrin β3 tail. Although the binding requirements in the β3 cytoplasmic domain were very similar for Pyk2 and for paxillin, we excluded the possibility that Pyk2 binds via paxillin to the β3 tail (Fig. 6D). By using GST-fusion proteins, we obtained additional evidence indicating that both interactions are indeed independent and direct (Fig. 7). However, the requirements for β3 tail binding to paxillin and Pyk2 differed strongly from its binding to talin. This was expected, as talin binding requires more membrane-proximal regions of integrin β tails, which are absent in our synthetic peptides (Tapley et al., 1989; Patil et al., 1999).

We further show that neither paxillin nor Pyk2 binding to peptides containing the C-terminal 17 amino acids of the integrin β3 cytoplasmic domain are altered by their cell adhesion-triggered tyrosine phosphorylation (Fig. 6C). Therefore, tyrosine phosphorylation of paxillin and Pyk2 is

unlikely to provide a direct regulatory cue for their binding to the β3 integrin cytoplasmic domain. This binding has then to be regulated by other means, for example by the availability of free β3 tails. Previous studies indicate indeed that the availability of integrin β tails for cytoskeletal interactions is constrained in unoccupied integrins. This constraint involves integrin α tails and it is released during binding of the extracellular ligand (LaFlamme et al., 1992; Briesewitz et al., 1993; Ylänne et al., 1993). Pyk2- and paxillin-binding to the integrin β3 tail could thus trigger their recruitment to β3 integrin-dependent cell contacts. A major current issue will now be to study the role of this novel interaction observed primarily in a cell-free system in the context of intact cells.

On the basis of these observations, podosomes emerge as dynamic cytoskeletal structures with many molecular and functional homologies to focal adhesions. Both adhesion structures use a similar set of adhesion receptors and of adaptor proteins that link the extracellular contact to the actin cytoskeleton as well as to signal transduction pathways. The tyrosine kinase Pyk2, which is normally absent in focal adhesions (Schaller and Sasaki, 1997), could functionally replace in podosomes the focal adhesion kinase FAK, which is only weakly expressed in osteoclasts and in cells of the monocytic lineage (Duong et al., 1998; Lin et al., 1994; Li et al., 1998). The integrin αVβ3, which is highly expressed during later stages of osteoclast differentiation, might be important to adapt podosomes to their function in osteoclast migration on bone and in the formation of the sealing zone during bone resorption (McHugh et al., 2000). Finally, the molecular complex that contains paxillin and Pyk2 bound to the C terminus of the integrin β3 chain could represent a molecular core structure that governs the distribution of regulatory cues linking integrin-dependent cell adhesion to podosome functions in osteoclasts.

We kindly acknowledge the expert help of Damien Ficheux (Institut de Biologie et Chimie des Protéines, Lyon) during the synthesis and characterization of peptides, and of Wilfried Condemine during the preparation of recombinant GST-paxillin. We are grateful to Mark Ginsberg, David Calderwood, Shouchun Liu and David Schlaepfer (The Scripps Research Institute, La Jolla, CA), Ravi Salgia (Dana-Farber Cancer Institute, Boston, MA), Michael Horton (London, UK), and to Immunex (Seattle, WA) for providing reagents.

REFERENCES

Anderson, D., Maraskovsky, E., Billinglsey, W. L., Dougall, W. C., Tometsko, M. E., Roux, E. R., Teepe, M. C., DuBose, R. F., Cosman, D. and Galibert, L. (1997). A homologue of the TNF receptor and its ligand enhance T-cell growth and dendritic cell function. *Nature* **390**, 175-179.

Blavier, L. and Delaissé, J. M. (1995). Matrix metalloproteinases are obligatory for the migration of preosteoclasts to the developing marrow cavity of primitive long bones. *J. Cell Sci.* **108**, 3649-3659.

Boissy, P., Machuca, I., Pfaff, M., Ficheux, D. and Jurdic, P. (1998). Aggregation of mononucleated precursors triggers cell surface expression of αVβ3 integrin, essential to formation of osteoclast-like multinucleated cells. *J Cell Sci.* **111**, 2563-2574.

Bretscher, A. (1981). Fimbrin is a cytoskeletal protein that crosslinks F-actin in vitro. *Proc. Natl. Acad. Sci. USA* **78**, 6849-6853.

Briesewitz, R., Kern, A. and Marcantonio, E. E. (1993). Ligand-dependent and -independent integrin focal contact localization: the role of the α chain cytoplasmic domain. *Mol. Biol. Cell* **4**, 593-604.

Burridge, K. and Chrzanowska-Wodnicka, M. (1996). Focal adhesions, contractility, and signaling. *Annu. Rev. Cell Dev. Biol*. **12**, 463-518.

Calderwood, D., Zent, R., Grant, R,. Rees, D.J.G., Hynes, R. O. and Ginsberg, M. H. (1999). The talin head domain binds to integrin β subunit cytoplasmic tails and regulates integrin activation. *J. Biol. Chem*. **274**, 28071-28074.

Carley, W., Bretscher A. and Webb, W. W. (1986). F-actin aggregates in transformed cells contain α-actinin and fimbrin but apparently lack tropomyosin. *Eur. J. Cell Biol*. **39**, 313-320.

Chellaiah, M., Kizer, N., Silva, M., Alvarez, U., Kwiatkowski, D. and Hruska, K. A. (2000). Gelsolin deficiency blocks podosome assembly and produces increased bone mass and strength. *J. Cell Biol*. **148**, 665-678.

Chen, W.-T. (1989). Proteolytic activity of specialized surface protrusions formed at rosette contact sites of transformed cells. *J. Exp. Zool*. **251**, 167-185.

Chen, W.-T., Olden, K., Bernard, B. A. and Chu, F.-F. (1984). Expression of transformation-associated protease(s) that degrade fibronectin at cell contact sites. *J. Cell Biol*. **98**, 1546-1555.

Chen, Y.-P., Djaffar, D., Pidard, D., Steiner, B., Cieutat, A.-M., Caen, J. P. and Rosa, J.-P. (1992). Ser752-Pro mutation in the cytoplasmic domain of integrin β3 subunit and defective activation of platelet integrin aIIbβ3 (glycoprotein IIbIIIa) in a variant of Glanzmann thrombasthenia. *Proc. Natl. Acad. Sci. USA* **89**, 10169-10173.

David-Pfeuty, T. and Singer, S. J. (1980). Altered distributions of the cytoskeletal proteins vinculin and α-actinin in cultured fibroblasts transformed by Rous sarcoma virus. *Proc. Natl. Acad. Sci. USA* **77**, 6687-6691.

Derossi, D., Joliot, A. H., Chassaing, G. and Prochiantz, A. (1994). The third helix of the Antennapedia homeodomain translocates through biological membranes. *J. Biol. Chem*. **269**, 10444-10450.

Duong, L., Lakkakorpi, P. T., Nakamura, I., Nagy, R. M. and Rodan, G. A. (1998). Pyk2 in osteoclasts is an adhesion kinase, localized in the sealing zone, activated by ligation of αVβ3 integrin, and phosphorylated by src kinase. *J. Clin. Invest*. **102**, 881-892.

Helfrich, M. H., Nesbitt, S. A., Lakkakorpi, P. T., Barnes, M. J., Bodary, S. C., Shankar, G., Mason, W. T., Mendrick, D. L., Väänänen, H. K. and Horton, M. A. (1996). β1 integrins and osteoclast function: involvement in collagen recognition and bone resorption. *Bone* **19**, 317-328.

Hynes, R. O. (1992). Integrins: versatility, modulation, and signaling in cell adhesion. *Cell* **69**, 11-25.

Jockusch, B. M., Bubeck, P., Giehl, K., Kroemker, M., Moschner, J., Rothkegel, M., Rüdiger, M., Schlüter, K., Stanke, G. and Winkler, J. (1995). The molecular architecture of focal adhesions. *Annu. Rev. Cell Dev. Biol*. **11**, 379-416.

Johansson, M. W., Larsson, E., Lüning, B., Pasquale, E.B. and Ruoslahti, E. (1994). Altered localization and cytoplasmic domain-binding properties of tyrosine-phosphorylated β1 integrin. *J. Cell Biol*. **126**, 1299-1309.

LaFlamme, S., Akiyama, S. K. and Yamada, K. M. (1992). Regulation of fibronectin receptor distribution. *J. Cell Biol*. **117**, 437-447.

Lakkakorpi, P., Horton, M. A., Helfrich, M. H., Karhukorpi, E. K. and Väänänen, H. K. (1991). Vitronectin receptor has a role in bone resorption, but does not mediate tight sealing zone attachment of osteoclasts to the bone surface. *J. Cell Biol*. **115**, 1179-1186.

Lakkakorpi, P., Nakamura, I., Nagy, R. M., Parsons, J. T., Rodan, G. A. and Duong, L. T. (1999). Stable association of PYK2 and p130cas in osteoclasts and their co-localization in the sealing zone. *J. Biol. Chem*. **274**, 4900-4907.

Li, X., Hunter, D., Morris, J., Haskill, J. S. and Earp, H. S. (1998). A calcium-dependent tyrosine kinase splice variant in human monocytes. *J. Biol. Chem*. **273**, 9361-9364.

Lin, T.H., Yurochko, A., Kornberg, L., Morris, J., Walker, J. J., Haskill, S. and Juliano, R. L. (1994). The role of protein tyrosine phosphorylation in integrin-mediated gene induction in monocytes. *J. Cell Biol*. **126**, 1585-1593.

Linder, S., Nelson, D., Weiss, M. and Aepfelbacher, M. (1999). Wiskott-Aldrich syndrome protein regulates podosomes in primary human macrophages. *Proc. Natl. Acad. Sci. USA* **96**, 9648-9653.

Marchisio, P., Cirillo, D., Naldini, L., Primavera, M. V., Teti, A. and Zambonin-Zallone, A. (1984). Cell substratum interaction of cultured avian osteoclasts is mediated by specific adhesion structures. *J. Cell Biol*. **99**, 1696-1705.

Marchisio, P., Cirillo, D., Teti, A., Zambonin-Zallone,A. and Tarone, G. (1987). Rous Sarcoma virus-transformed fibroblasts and cells of monocytic origin display a peculiar dot-like organization of cytoskeletal proteins involved in microfilament-membrane interaction. *Exp. Cell Res*. **169**, 202-214.

Marchisio, P., Bergui, L., Corbascio, G.C., Cremona, O., D'Urso, N.,

Schena, M., Tesio, L. and Caligaris-Cappio, F. (1988). Vinculin, talin, and integrins are localized at specific adhesion sites of malignant B-lymphocytes. *Blood* **72**, 830-833.

McHugh, K., Hodivala-Dilke, K., Zheng, M.-H., Namba, N., Lam, J., Novack, D., Feng X., Ross, F. P., Hynes, R. O. and Teitelbaum, S. L. (2000). Mice lacking β3 integrins are osteosclerotic because of dysfunctional osteoclasts. *J. Clin. Invest*. **105**, 433-440.

Nakamura, I., Pilkington, M. F., Lakkakorpi, P. T., Lipfert, L., Sims, S.M., Dixon, S. J., Rodan, G. A. and Duong, L.T. (1999). Role of aVβ3 integrin in osteoclast migration and formation of the sealing zone. *J. Cell Sci*. **112**, 3985-3993.

Nitsch, L., Gionti, E., Cancedda, R. and Marchisio, P. C. (1989). The podosomes of Rous Sarcoma virus transformed chondrocytes show peculiar ultrastructural organization. *Cell Biol. Int. Rep*. **13**, 919-926.

Ochoa, G.-C., Sepnev, V. I., Neff, L., Ringstad, N., Takei, K., Daniel, L., Kim, W., Cao, H., McNiven, M., Baron, R. and De Camilli, P. (2000). A functional link between dynamin and the actin cytoskeleton at podosomes. *J. Cell Biol*. **150**, 377-389.

O'Toole, T. E., Ylänne, J. and Culley, B. M. (1995). Regulation of integrin affinity states through an NPXY motif in the β subunit cytoplasmic domain. *J Biol Chem*. **270**, 8553-8558.

Patil, S., Jedsadayanmata, A., Wencel-Drake, J. D., Wang, W., Knezevic, I. and Lam, S. C.-T. (1999). Identification of a talin-binding site in the integrin β3 subunit distinct from the NPLY regulatory motif of post-ligand binding functions: the talin N-terminal head domain interacts with the membrane-proximal region of the β3 cytoplasmic tail. *J. Biol. Chem*. **274**, 28575-28583.

Pfaff, M., Liu, S., Erle, D. J. and Ginsberg, M. H. (1998). Integrin β cytoplasmic domains differentially bind to cytoskeletal proteins. *J. Biol. Chem*. **273**, 6104-6109.

Quinn, J., Elliott, J., Gillespie, M. T. and Martin, T. J. (1998). A combination of osteoclast differentiation factor and macrophage-colony stimulating factor is sufficient for both human and mouse osteoclast formation in vitro. *Endocrinology* **139**, 4424-4427.

Rottner, K., Hall, A. and Small, J. V. (1999). Interplay between Rac and Rho in the control of substrate contact dynamics. *Curr. Biol*. **9**, 640-648.

Sabe, H., Hata, A., Okada, M., Nakagawa, H. and Hanafusa, H. (1994). Analysis of the binding of the src homology 2 domain of csk to tyrosine tyrosine-phosphorylated proteins in the suppression and mitotic activation of c-src. *Proc. Natl. Acad. Sci. USA* **91**, 3984-3988.

Sato, T., del Carmen Ovejero, M., Hou, P., Heegaard, A.-M., Kumegawa, M., Foged, N. T. and Delaissé, J.-M. (1997). Identification of membrane-type matrix metalloproteinase MT1-MMP in osteoclasts. *J. Cell Sci*. **110**, 589-596.

Schaffner-Reckinger, E., Gouon, V., Melchior, C., Plançon, S. and Kieffer, N. (1998). Distinct involvment of β3 integrin cytoplasmic domain tyrosine residues 747 and 759 in integrin-mediated cytoskeletal assembly and phosphotyrosine signaling. *J. Biol. Chem*. **273**, 12623-12632.

Schaller, M. and Sasaki, T. (1997). Differential signaling by the focal adhesion kinase and cell adhesion kinase β. *J. Biol. Chem*. **272**, 25319-25325.

Schaller, M. D., Otey, C. A., Hildebrand, J. D. and Parsons, J. T. (1995). Focal adhesion kinase and paxillin bind to peptides mimicking β integrin cytoplasmic domains. *J. Cell Biol*. **130**, 1181-1187.

Shen, Y., Schneider, G., Cloutier, J.-F., Veillette, A. and Schaller, M. D. (1998). Direct association of protein-tyrosine phosphatase PTP-PEST with paxillin. *J. Biol Chem*. **273**, 6474-6481.

Sieg, D., Hauck, C. R., Ilic, D., Klingbeil, C. K., Schaefer, E., Damsky, C. H. and Schlaepfer, D. D. (2000). FAK integrates growth-factor and integrin signals to promote cell migration. *Nat. Cell Biol*. **2**, 240-256.

Solari, F., Domenget, C., Gire, V., Woods, C., Lazarides, E., Rousset, B. and Jurdic, P. (1995). Multinucleated cells can continuously generate mononucleated cells in the absence of mitosis: a study of cells of the avian osteoclast lineage. *J. Cell Sci.* **108**, 3233-3241.

Stickel, S. and Wang, Y.-L. (1987). Alpha-actinin-containing aggregates in transformed cells are highly dynamic structures. *J. Cell Biol*. **104**, 1521-1526.

Tanaka, T., Yamaguchi, R., Sabe, H., Sekiguchi, K. and Healy, J. M. (1996). Paxillin association in vitro with integrin cytoplasmic domain peptides. *FEBS Lett.* **399**, 53-58.

Tapley, P., Horwitz, A., Buck, C., Duggan, K. and Rohrschneider, L. (1989). Integrins isolated from Rous sarcoma virus-transformed chicken embryo fibroblasts. *Oncogene* **4**, 325-333.

Tarone, G., Cirillo, D., Giancotti, F. G., Comoglio, P. M. and Marchisio, P. C. (1985). Rous sarcoma virus-transformed fibroblasts adhere primarily at discrete protrusions of the ventral membrane called podosomes. *Exp. Cell Res*. **159**, 141-157.

Turner, C. (1994). Paxillin: a cytoskeletal target for tyrosine kinases. *BioEssays* **16**, 47-52.

Turner, C. and Miller, J. T. (1994). Primary sequence of paxillin contains putative SH2 and SH3 domain binding motifs and multiple LIM domains: identification of a vinculin and pp125FAK binding region. *J. Cell Sci.* **107**, 1583-1591.

Turner, C., Brown, M. C., Perrotta, J. A., Riedy, M. C., Nikolopoulos, S. N., McDonald, A. R., Bagrodia, S., Thomas, S. and Leventhal, P. S. (1999). Paxillin LD4 motif binds PAK and PIX through a novel 95-kD ankyrin repeat, ARF-GAP protein: a role in cytoskeletal remodeling. *J. Cell Biol*. **145**, 851-863.

Väänänen, H. K. and Horton, M. (1995). The osteoclast clear zone is a specialized cell-extracellular matrix adhesion structure. *J. Cell Sci.* **108**, 2729-2732.

Väänänen, H., Zhao, H., Mulari, M. and Halleen, J. M. (2000). The cell biology of osteoclast function. *J. Cell Sci.* **113**, 377-381.

Wang, E., Yin, H. L., Krueger, J. G., Caliguiri, L. A. and Tamm, I. (1984). Unphosphorylated gelsolin is localized in regions of cell-substratum contact or attachment of Rous sarcoma virus-transformed rat cells. *J. Cell Biol*. **98**, 761-771.

Weng, Z., Taylor, J. A., Turner, C. E., Brugge, J. S. and Seidel-Dugan, C. (1993). Detection of src homology 3-binding proteins, including paxillin, in normal and v-src-transformed Balb/c 3T3 cells. *J. Biol. Chem*. **268**, 14956-14963.

Yasuda, H., Shima, N., Nakagawa, N., Yamaguchi, K., Kinosaki, M., A. Mochizuki, Yano, K., Goto, M., Murakami, A., Tsuda, E. et al. (1998). Osteoclast differentiaton factor is a ligand for osteoprotegerin/osteoclastogenesis-inhibitory factor and is identical to TRANCE/RANKL. *Proc. Natl. Acad. Sci. USA* **95**, 3597-3602.

Yin, H. (1987). Gelsolin: calcium- and polyphosphoinositide-regulated actin-modulating protein. *BioEssays* **7**, 176-179.

Ylänne, J., Chen, Y., O'Toole, T. E., Loftus, J. C., Takada, Y. and Ginsberg, M. H. (1993). Distinct functions of integrin α and β subunit cytoplasmic domains in cell spreading and formation of focal adhesions. *J. Cell Biol*. **122**, 223-233.

Ylänne, J., Huuskonen, J., O'Toole, T. E., Ginsberg, M. H., Virtanen, I. and Gahmberg, C. G. (1995). Mutation of the cytoplasmic domain of the integrin β3 subunit. *J. Biol. Chem*. **270**, 9550-9557.

Zambonin-Zallone, A., Teti, A., Grano, M., Rubinacci, A., Abbadini, M., Gaboli, M. and Marchisio, P. C. (1989). Immunocytochemical distribution of extracellular matrix receptors in human osteoclasts: a β3 integrin is colocalized with vinculin and talin in podosomes of osteoclastoma giant cells. *Exp. Cell Res*. **182**, 645-652.